The 2015 World Congress on
Advances in Civil, Environmental, and Materials Research (ACEM15)
Incheon, Korea, August 25-29, 2015

The Thermo-Mechanical Behavior of Micro Circular Diaphragm Measured by means of the Bulge Test Technique

*Wael A. Al-Tabey[1)]

Department of Mechanical Engineering, Alexandria University,
Alexandria (21544), Egypt
wael.altabey@gmail.com

ABSTRACT

The objective of this paper is to determine the thermo-mechanical behavior of micro circular diaphragm, used in numerous engineering and bioengineering sensors applications by using the bulge test technique. The specimen is first pre-stressed and then clamped between two plates. A differential pressure is leading to a deformation of the circular diaphragm. Analytical formulate of bulge test technique for circular diaphragm thermo-mechanical characterisation was established. This makes the plane-strain bulge test ideal for studying the mechanical behavior of diaphragm in both the elastic and plastic regimes. A finite element model (FEM) can be extended to apply for the bulge test of circular diaphragm and study the effect of pre-stress on pressure test and compare between the (FEM) and another one from analytical calculus. Differential specimen thickness and materials were to describe the mechanical behavior of the circular diaphragm under deformation. The temperature effect on the material properties of circular diaphragm was discussed in this work for studying the thermo-mechanical behavior of diaphragm. The simulation results were obtained using MATLAB software and MATLAB PDE tool box.

1. INTRODUCTION

Many of the materials that are used for thin films are quite common, with well-known and documented material properties. So why is it important to spend so much time and money on the analysis and research of these films? It is not quite so easy (Saute 2000). There has been, however, no systematic study of the accuracy of these formulae in the plastic regime. In this study, we first review the equations used to analyze bulge test results. Then, a finite element analysis is carried out to verify the accuracy of these equations in the plastic regime.

The hydrostatic bulging of metal sheets, more commonly known as the bulge test, is a preferred method for the determination of the strain-hardening characteristics of metals. Numerous works to predict the behavior and characteristics of metals under bulging have been undertaken and reported in the literature, the works of Hill (1950) and Mellor (1956) on the bulging of circular diaphragms being the earlier contributions in this field. (Swift 1952) examined the conditions for instability of plastic strain under

[1)] Assistant Professor

plane stress for a Plane Stress of Sheffield material conforming to the Mises-Hencky yield condition and strain-hardening according to a unique relationship between root mean-square values of shear stress and incremental strain for circular thin film. (Chater and Neale 1983) examined the large strain behaviour of a circular membrane under uniform hydrostatic pressure for materials with transversely isotropic plastic properties. A variational principle is first applied to derive the governing equations for the pressurized membrane. (Storakers 1966) presented an analysis of the plastic deformation including instability phenomena of a circular membrane subject to one-sided hydrostatic pressure. Equations determining stresses and strains are given for the deformation process of materials with a parabolic stress-strain curve. Numerical solutions have been carried out for some special cases. Comparison is made with theoretical and experimental results obtained by other investigators. (Zeghloul 1991) examined the plastic bulging of pressurized circular membranes with particular attention to the effect of material parameters on the inherent in homogeneity of the test. (Wang and Shammamy 1969) are analyzed the hydrostatic bulging of a circular sheet clamped on the basis of both an incremental theory and the corresponding total strain theory of plasticity. The material of the sheet is assumed to have strain-hardening capacity and to be anisotropic in the thickness direction. (Ilahi and et al. 1981) presented a numerical method of solution for the plastic deformation of a circular metal diaphragm. The analysis is applied to the bulging of soft commercial purity aluminum sheet and the results correlated with experiment.

The accuracy and reliability of the bulge test has been analyzed by a number of researchers. (Itozaki 1982) showed that failure to include the initial height of the membrane in the analysis leads to an apparent nonlinear elastic behavior of the film. (Small et al. 1992) analyzed the influence of initial film conditions such as film wrinkling, residual stress, and initial height of the membrane using finite element analysis. (Vlassak 1994) investigated the contribution of the film bending stiffness to the deflection of a membrane. He showed that for typical bulge test geometries, the bending moment is only significant very close to the edge of the membrane and is negligible everywhere else.

The plane-strain bulge test is a powerful new technique for measuring the mechanical properties of thin films. In this technique, the stress–strain curve of a thin film is determined from the pressure-deflection behavior of the circular membrane made of the film of interest, see Fig. 1. For a thin membrane in a state of plane strain, film stress and stain are distributed uniformly across the membrane width, and simple analytical formulae for stress and strain can be established (Xiang et al. 2005).

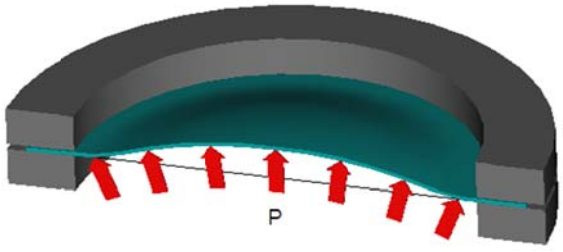

Fig. 1 Schematic representation of the bulge test

2. GEOMETRICAL MODEL

Fig. 2(a) represents the geometrical model of micro circular diaphragm before and after displacement at left half and right half side respectively. As shown in the figure the micro circular diaphragm has a radius *a* and the thickness *h*.

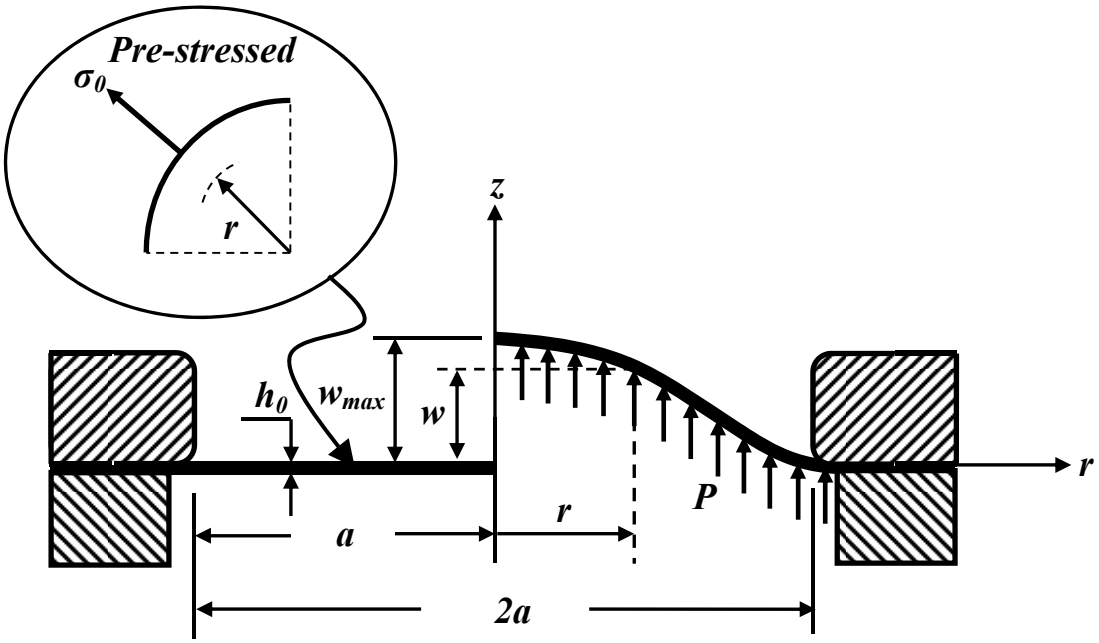

(a) The geometrical model element

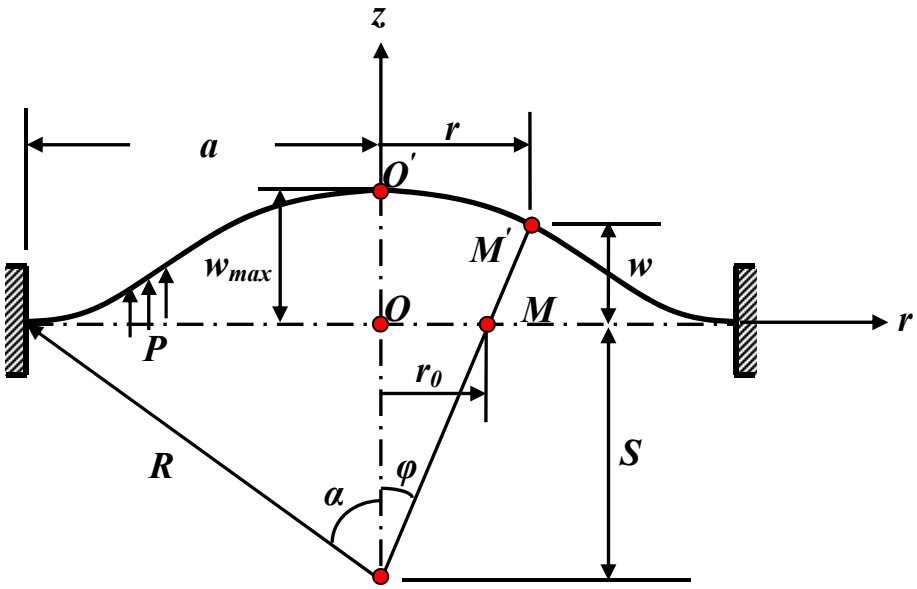

(b) Schematic of deformation modeling

Fig. 2 The model of micro circular diaphragm

The diaphragm is first pre-stress under radial stress σ_0 to ensure the initial deflection before applied the load equal zero and then clamped between two plates. The upper side of the plate is exposed to room temperature T_t = 25 Cº and the lower side of the film is subjected to thermo-fluid media with pressure P and temperature T_b. Fig. 2(b) represents the dome profile of the diaphragm deformation.

3. FORMULATION

The equation of motion governing the circular diaphragm under the assumption of the classical deformation theory in terms of the plate deflection *W(x, y, t)* is given by:

$$\frac{\partial^2 m_r}{\partial r^2} - \frac{2}{r}\frac{\partial^2 m_{rt}}{\partial r \partial \theta} + \frac{\partial^2 m_t}{\partial \theta^2} = -\rho h \frac{\partial^2 w}{\partial t^2} \tag{1}$$

Where *w* is the transverse deflection, *ρ* = the density per unit area of the plate and *h* is the circular diaphragm thickness at any point could be calculated from the geometry shape of Fig. 2 by equations:

$$\mathrm{h} = \mathrm{h}_0 \left(\frac{\sin\alpha}{\alpha}\right)^2 \left(\frac{\varphi}{\sin\varphi}\right) \tag{2}$$

$$\alpha = \sin^{-1}\left(\frac{\mathrm{a}}{\mathrm{R}}\right) \tag{3}$$

$$\varphi = \tan^{-1}\left(\frac{\mathrm{r}}{\mathrm{S}}\right) \tag{4}$$

The radius of curvature R, see Fig. 2, is:

$$\mathrm{R} = \frac{\mathrm{a}^2 + \mathrm{w}_{\max}}{2\mathrm{w}_{\max}} \tag{5}$$

$$\mathrm{S} = \frac{\mathrm{a}}{\tan\alpha} \tag{6}$$

The bending and twisting moments ($\mathrm{m_r}$, $\mathrm{m_t}$, $\mathrm{m_{rt}}$) and shear forces ($\mathrm{q_r}$, $\mathrm{q_t}$) in terms of displacements and thermal effect term we can be written in the following form:

$$\left.\begin{aligned}
m_r &= -D\left[\frac{\partial^2 w}{\partial r^2} + \upsilon\left(\frac{1}{r}\frac{\partial w}{\partial r} + \frac{1}{r^2}\frac{\partial^2 w}{\partial \theta^2}\right) + \alpha_T \frac{\Delta T}{h}(1-\upsilon)\right] \\
m_t &= -D\left[\frac{1}{r}\frac{\partial w}{\partial r} + \frac{1}{r^2}\frac{\partial^2 w}{\partial \theta^2} + \upsilon\frac{\partial^2 w}{\partial r^2} + \alpha_T \frac{\Delta T}{h}(1-\upsilon)\right] \\
m_{rt} &= m_{tr} = -D(1-\upsilon)\left(\frac{1}{r}\frac{\partial^2 w}{\partial r \partial \theta} - \frac{1}{r^2}\frac{\partial w}{\partial \theta}\right) \\
q_r &= -D\frac{\partial}{\partial r}(\nabla_r^2 w) - \frac{\partial m_T}{\partial r} \\
q_t &= -D\frac{1}{r}\frac{\partial}{\partial \theta}(\nabla_r^2 w) - \frac{\partial m_T}{\partial \theta}
\end{aligned}\right\} \tag{7}$$

Similarly, the formulas for the plane stress components of the circular diaphragm, from Equation (7) are written in the following form:

$$\sigma_r = \frac{12m_r}{h^3}z, \quad \sigma_t = \frac{12m_t}{h^3}z, \quad \tau_{rt} = \tau_{tr} = \frac{12m_{tr}}{h^3}z \tag{8}$$

The flexural rigiditie D of the plate is given by:

$$D = \frac{Eh^3}{12(1-\upsilon^2)} \tag{9}$$

Where *E* are the young's moduli, υ is the poisson's ratio. Thus, the governing partial differential equation of the micro circular diaphragm subjected to thermal and mechanical load as shown in Fig. 1 is reduced to:

$$\nabla_r^4 w \equiv \frac{\partial^4 w}{\partial r^4} + \frac{2}{r}\frac{\partial^3 w}{\partial r^3} - \frac{1}{r^2}\frac{\partial^2 w}{\partial r^2} + \frac{1}{r^3}\frac{\partial w}{\partial r} + \frac{2}{r^2}\frac{\partial^4 w}{\partial r^2 \partial \theta^2} - \frac{2}{r^3}\frac{\partial^3 w}{\partial \theta^2 \partial r} + \frac{4}{r^4}\frac{\partial^2 w}{\partial \theta^2} + \frac{1}{r^4}\frac{\partial^4 w}{\partial \theta^4} = \frac{P+P_T}{D} \tag{10}$$

Where P_T is the thermal load applied on circular diaphragm is given by:

$$P_T = \nabla_r^2 m_T \tag{11}$$

Where $\nabla_r^2 = \left(\frac{\partial^2}{\partial r^2} + \frac{1}{r}\frac{\partial}{\partial r} + \frac{1}{r^2}\frac{\partial^2}{\partial \theta^2}\right)$ and m_T is the thermal equivalent bending moment, it is obtained by equation:

$$m_T = \frac{\alpha_T E}{(1-\upsilon)}\int_{-(h/2)}^{+(h/2)} \Delta T z dz = D\alpha_T \frac{T_t - T_b}{h}(1+\upsilon) \tag{12}$$

3.1 The Circular Diaphragm Pre-stress Modeling

Considering the pre-existence of an equi-biaxial residual stress per unit length σ_0 before applying the load on the micro circular diaphragm at radial direction to ensure that the deflection $w_0=0$ as shown on the Fig. 3, the pre-stress must be placed in the equation of the radial stress before calculating $\mathrm{m_r}$.

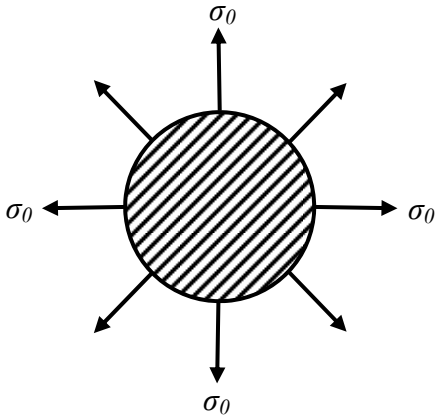

Fig. 3 The pre-stress of micro circular diaphragm model

From the previous equations for m_r and σ_r of circular diaphragm we can be written these after added the pre-stress term in the following form:

$$\sigma_r = -z\left(\frac{E}{(1-\upsilon^2)}\left[\frac{\partial^2 w}{\partial r^2} + \upsilon\left(\frac{1}{r}\frac{\partial w}{\partial r} + \frac{1}{r^2}\frac{\partial^2 w}{\partial \theta^2}\right) + \alpha_T \frac{\Delta T}{h}(1-\upsilon)\right] + \frac{\sigma_0}{(1-\upsilon)}\right) \tag{13}$$

$$m_r = \int_{-(h/2)}^{+(h/2)} \sigma_r z dz = -D\left[\frac{\partial^2 w}{\partial r^2} + \upsilon\left(\frac{1}{r}\frac{\partial w}{\partial r} + \frac{1}{r^2}\frac{\partial^2 w}{\partial \theta^2}\right) + \alpha_T \frac{\Delta T}{h}(1-\upsilon)\right] + \frac{h^3\sigma_0}{12(1-\upsilon)} \tag{14}$$

4. METHOD OF SOLUTION

When an applied loading and end restraints of the micro circular diaphragm are independent of the angle φ then the deflection of the diaphragm and the stress resultants and stress couples will depend upon the radial position r only. Such a bending of the circular diaphragm is referred to as axially symmetrical and the following simplifications can be made:

$$\frac{\partial^k ()}{\partial \theta^k} = m_{rt} = q_t = 0; \quad k = 1,2,3,4 \tag{15}$$

The differential equation of the deflected surface of the circular plate, Equation (10), reduces now to:

$$\frac{d^4 w}{dr^4} + \frac{2}{r}\frac{d^3 w}{dr^3} - \frac{1}{r^2}\frac{d^2 w}{dr^2} + \frac{1}{r^3}\frac{dw}{dr} = \frac{P+P_T}{D} \tag{16}$$

Eq. (16) appears in the form:

$$\frac{1}{r}\frac{d}{dr}\left\{\frac{1}{r}\frac{d}{dr}\left[\frac{1}{r}\frac{d}{dr}\left(r\frac{dw}{dr}\right)\right]\right\} = \frac{P+P_T}{D} \tag{17}$$

Where Eq. (17) the governing partial differential equation of the axisymmetric thermo-mechanical bending of circular diaphragm and *w* is the deflection of the diaphragm at axial direction we can be obtained by solve the partial differential Eq. (17).

Rigorous solution of Eq. (17) is obtained as the sum of the complementary solution of the homogeneous differential equation, w_h, and the particular solution, w_p, i.e.,

$$w = w_h + w_p \tag{18}$$

The complementary solution of Equation (17) is given by:

$$w_h = C_1 \ln r + C_2 r^2 \ln r + C_3 r^2 + C_4 \tag{19}$$

Where $C_i\,(i = 1,2,3,4)$ are constants that can be evaluated from the boundary conditions. The particular solution, w_p, is obtained by successive integration of Eq. (17):

$$w_p = \int \frac{1}{r}\int r \int \frac{1}{r}\int \frac{r(P(r)+P_T(r))}{D} drdrdrdr \tag{20}$$

4.1 The boundary conditions

The boundary conditions for micro circular diaphragm with clamped edge as shown in Fig.2 are:

$$\left.\begin{array}{l} w = 0|_{r=a} \\ \frac{\partial w}{\partial r} = 0\Big|_{a=0} \end{array}\right\} \tag{21}$$

For the solid plate, which contains no concentrated loads at *r=0*, it is easy to see that the terms involving the logarithms in Eq. (19) yield an infinite displacement and bending moment, and the shear force for all values of C_1 and C_2, except zero; therefore, $C_1 = C_2 = 0$. Thus, for a solid circular plate subjected to an axisymmetric distributed load with arbitrary boundary conditions, the deflection surface is given by:

$$\mathrm{w} = \mathrm{C}_3\mathrm{r}^2 + \mathrm{C}_4 + \mathrm{w}_\mathrm{p} \tag{22}$$

The constants of integration C_3 and C_4 in this equation are determined from boundary conditions and we obtain:

$$C_3 = -\frac{Pa^2}{32D} - \frac{m_T}{D}\left[\frac{1}{4}\ln a - \frac{1}{8}\right] \tag{23}$$

$$C_4 = \frac{Pa^4}{64D} + \frac{a^2 m_T}{8D} \tag{24}$$

And after some manipulation, the transverse deflection *w*, bending moments (m_r, m_t) and shear forces (q_r) will becomes:

$$w = \frac{P}{64D}(a^2 - r^2)^2 + \frac{m_T}{4D}r^2(\ln r - \ln a) + \frac{m_T}{8D}(a^2 - 3r^2) \tag{25}$$

$$m_r = \frac{P}{16}\left(a^2(\upsilon + 1) - r^2(3 + \upsilon)\right) + \frac{m_T}{2}(\upsilon + 1)(\ln a - \ln r) - \frac{m_T}{2} - D\alpha_T\frac{\Delta T}{h}(1 - \upsilon) + \frac{h^3\sigma_0}{12(1-\upsilon)} \tag{26}$$

$$m_t = \frac{P}{16}\left(a^2(\upsilon + 1) - r^2(1 + 3\upsilon)\right) + \frac{m_T}{2}(\upsilon + 1)(\ln a - \ln r) - \frac{m_T}{2}\upsilon - D\alpha_T\frac{\Delta T}{h}(1 - \upsilon) \tag{27}$$

$$q_r = -\frac{Pr}{2} \tag{28}$$

5. RESULTS AND DISCUSSION

In this section, some analytical numerical results are presented for micro circular diaphragm has the geometrical properties of 2a = 1 mm and about 0.1 mm thickness (see section (2)). The diaphragm is first pre-stress under radial stress σ_0 then clamped between two plates. The diaphragm is made of one of common material which used in numerous micro electro-mechanical sensors (memes) and bioengineering applications;

this material is pure aluminum which mechanical and thermal properties are given in Table 1. Table 2 show the mechanical and thermal Loading history applied on the micro Circular Diaphragm .

Table 1 Material thermal and mechanical properties

Material	**E (Gpa)**	**G (Gpa)**	**υ**	**K (W.C^{-1}. m^{-1})**	**α (C^{-1})**
Al-Pure	71.7	26.9	0.333	237	23 E-6

Table 2 Loading history

Pressure *P* (MPa)	P_1 = 100	P_2 = 200	P_3 = 300	P_4 = 400
Temperature T$_b$ (C$^\circ$)	T_1 = 50	T_2 = 100	T_3 = 150	T_4 = 200

5.1 Analytical Results

The mechanical behavior of micro circular diaphragm under the previous conditions that have been mentioned we can be discussed in Figs. 4-5. Figs. 4 (a)-(f) shows the relation between transverse deflection *w*, bending moments (m_r, m_t), shear force (q_r) and stress (S_r, S_t) respectively with the micro circular diaphragm radius (*r*) under varying pressure (*P*). As shown in the Fig. 4(a) the transverse deflection *w* is decreased with diaphragm radius (*r*) and increased with pressure (*P*) and the maximum deflection occurs at the center of the plate at *r=0*. Figs. 4(b)-(c) show the bending moment diagram of radial and tangential moment where increased with pressure (*P*) and the residual moment due to pre-stress is appear in the Fig. 4(b) and the maximum bending moment ($\mathrm{m_r}$, $\mathrm{m_t}$) are occurs at (*r = a, r = 0*) respectively. As shown in Fig. 4(d) the shear force (q_r) is increased with both diaphragm radius and pressure, and the maximum shear force occurs at the at the edge of the plate at *r = a*. Figs. 4(e)-(f) show the stress at radial and tangential direction of diaphragm where increased with pressure (*P*) and the pre-stress is appear in Fig. 4(e).

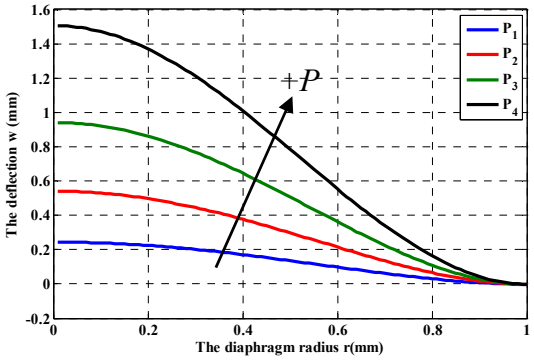

(a) Transverse deflection *w*

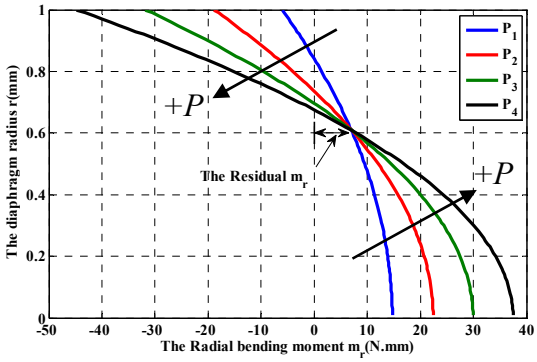

(b) Radial bending moment $\mathrm{m_r}$

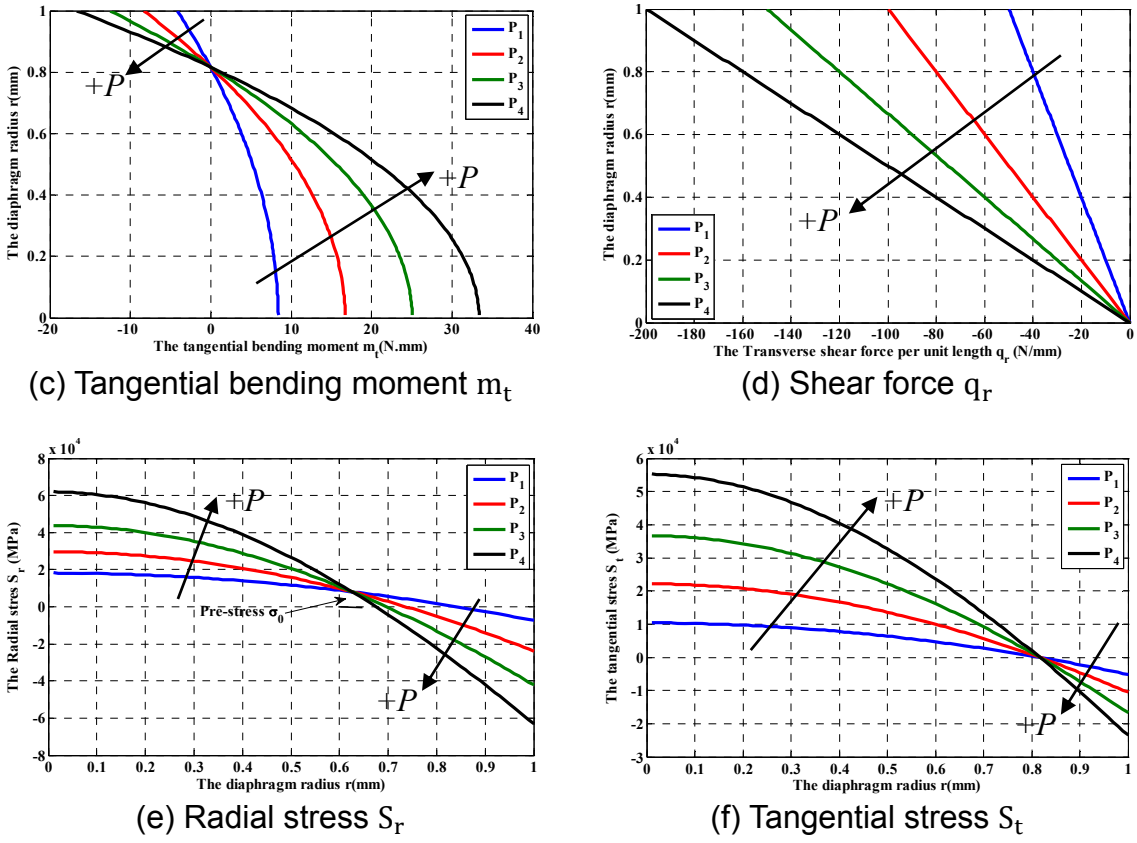

(c) Tangential bending moment $\mathrm{m_t}$ (d) Shear force $\mathrm{q_r}$

(e) Radial stress $\mathrm{S_r}$ (f) Tangential stress $\mathrm{S_t}$

Fig. 4 The relation between the micro circular diaphragm radius (*r*) and the mechanical characteristics under varying applying pressure (*P)* for all target material.

Fig. 5 shows the relation between the radial stress S_r and radial strain e_r , where the radial strain e_r is increased with radial stress S_r. This relation is very important in engineering analysis where the Young's modulus *E* of the diaphragm material from the slop of this liner relation.

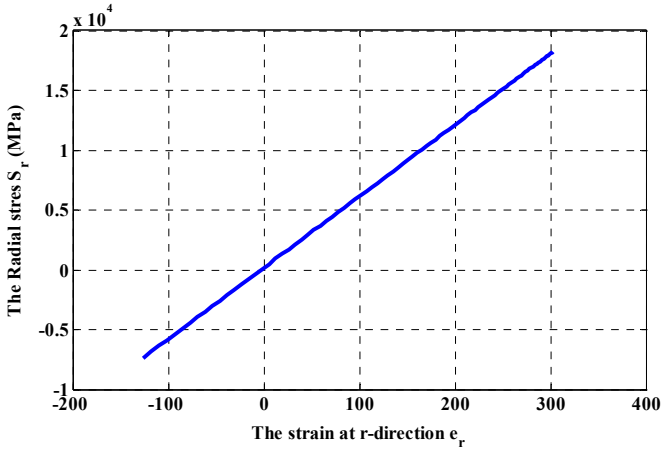

Fig. 5 The relation between the radial stress S_r and radial strain e_r

The thermal behavior of micro circular diaphragm under the previous conditions that have been mentioned we can be discussed in Fig. 6. Fig. 6(a)-(b) show the relation between bending moments (m_r, m_t) respectively with the micro circular diaphragm radius (r) under varying temperature (T_b), where the maximum bending moments are increased with temperature (T_b).

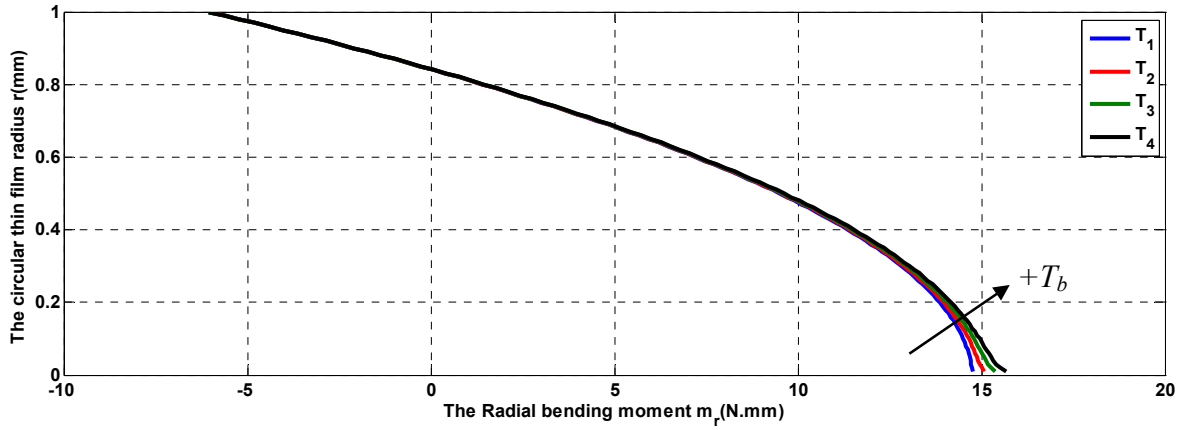

(a) Radial bending moment $\mathrm{m_r}$

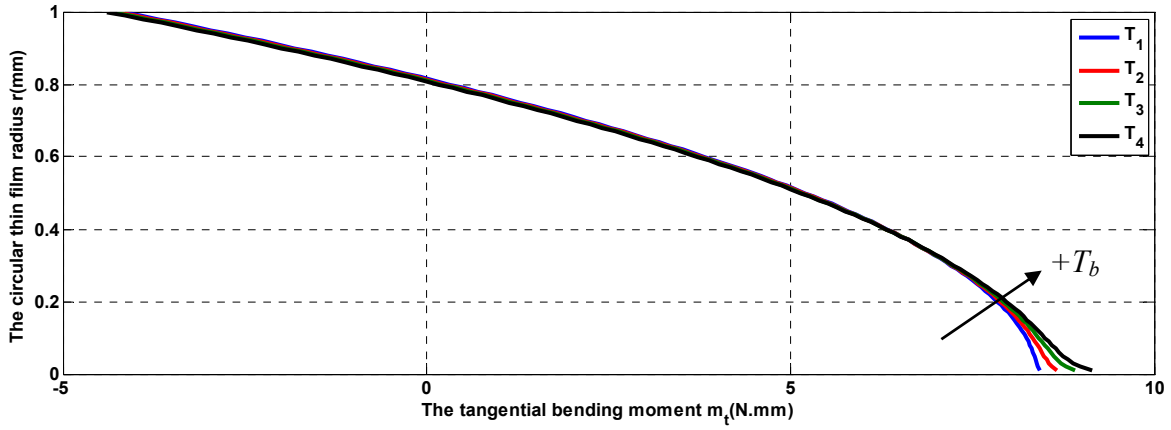

(b) Tangential bending moment $\mathrm{m_t}$

Fig. 6 The relation between the micro circular diaphragm radius (r) and the mechanical characteristics under varying temperature (T_b).

Thickness Deformation Fig. 7 shows the micro circular diaphragm thickness deformatio n behavior across the diaphragm radius (r) under varying pressure (P) and temperature (T_b). As shown in the Fig.5 (a) the dome thickness (h) is increased with diaphragm radi us r and decreased with pressure (P), the thickness strain e_h in the Fig. 7 (b)-(c) is incre ased with the pressure (P) and temperature (T_b) respectively.

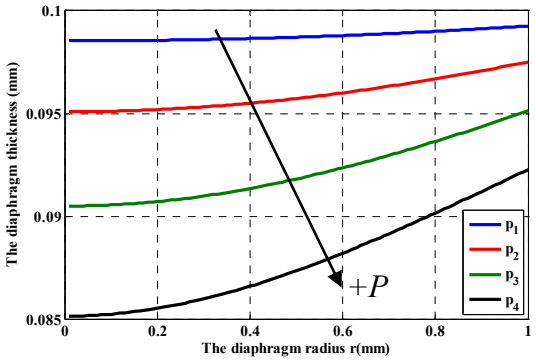

(a) The relation between dome thickness *h* and the diaphragm radius r under varying pressure *P*

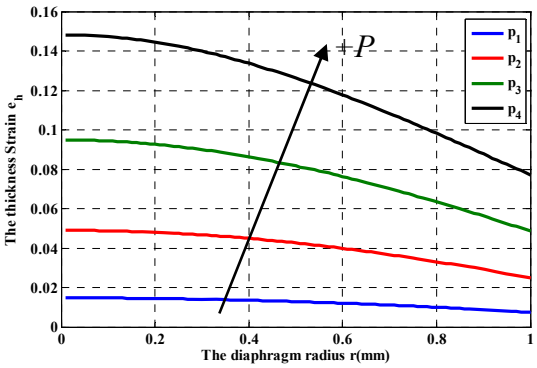

(b) The relation between the thickness strain e_h and the diaphragm radius r under varying pressure *P*

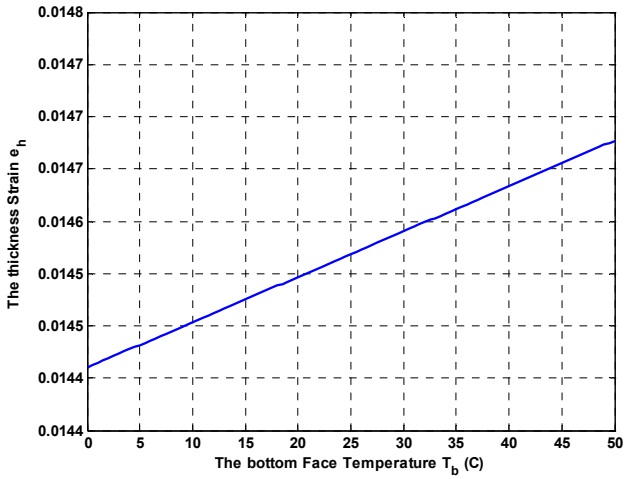

(c) The relation between the thickness strain e_h and the diaphragm bottom face temperature T_b

Fig. 7 The micro circular diaphragm thickness deformation behavior across the diaphra gm radius (*r*) under varying pressure (*P*) and temperature (T_b)

5.2 Numerical Results

The finite element simulation for the bulge test of micro circular diaphragm under the previous conditions that have been mentioned we can be discussed in Fig. 8. Fig. 8 shows the deformation history of micro circular diaphragm in both 3D Mesh mode and contour mode at applied pressure $P= P_1 = 100$ *MPa*. As shown in the Fig. 8 the maximum deflection occurs at the center of the plate at *r=0*, the maximum deflection w_{max} is found 0.24 mm. If we compared the maximum deflection from a finite element simulation model and another one from analytical calculus we are found that they are closed.

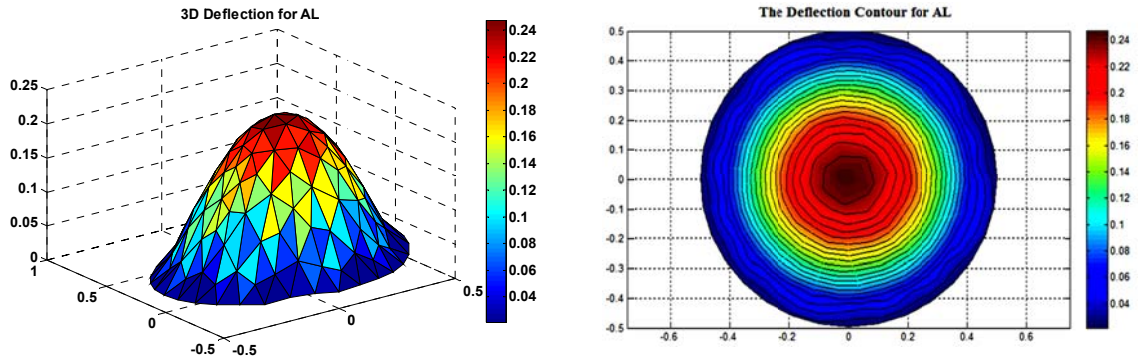

(a) 3D Mesh mode (b) Contour mode

Fig. 8 The finite element simulation for the bulge test of micro circular diaphragm by using MATLAB PDE tool box

6. CONCLUSION

In this paper, both analytical and numerical analysis of bulge test technique for micro circular diaphragm subjected to thermal and mechanical load has been shown. In the analytical analysis we have derived the partial differential equation of the micro circular diaphragm. The mechanical and thermal curves of the material flow is plotted and discussed. The thickness distribution across the diaphragm radius is discussed to describe the mechanical behavior of the micro circular diaphragm under deformation. The finite element simulation for the bulge test of micro circular diaphragm has been shown for the same conditions of the analytical calculus and the comparison between them has been to accuracy and validity of proposed technique. It was found from the results of the comparison the convergence is occurred between the finite element model and analytical model.

REFERENCES

Saute W., (2000), 'Thin Film Mechanics –Bulging And Stretching'. PhD thesis, Mechanical Engineering, University of Vermont.

Hill R., (1950), 'A theory of plastic bulging of a metal diaphragm by lateral pressure', Phil. Mag. (ser 7) 41.

Mellor P.B., (1956), Stretch forming under fluid pressure, J. Mech. Phys. Solids 5.

Swift H. W., (1952), 'Plastic instability under plane stress', J. Mechanics and Physics of Solids, Vol. 1, pp. 1 to 18.

Chater E. and Neale K. W., (1983), 'Finite plastic deformation of a circular membrane under hydrostatic pressure-I', J. Mech. Sci. Vol. 25, No. 4, pp. 219-233.

Storakers B., (1966), 'Finite plastic deformation of a circular membrane under hydrostatic pressure', J. Mech. Sci. Vol. 8, pp. 619-628.

Zeghloul A., Mesrar R. and Ferron G., (1991), 'Influence of material parameters on the hydrostatic bulging of a circular diaphragm', J. Mech. Scl. Vol. 33, No. 3, pp. 229-243.

Wang N. M. and Shammamy M. R., (1969), O'n the plastic bulging of a circular diaphragm by hydrostatic pressure', J.M ech.Ph ys. Solid1s, Vo1.7,pp 43-64.

Ilahi M. F., Parmar A. and Mellor P. B., (1981), 'Hydrostatic bulging of a circular aluminum diaphragm', Int. J. Mech. Sci. Vol. 23, pp. 221-227.

Itozaki H., (1982), 'Mechanical properties of composition modulated copper-palladium foils', Ph.D. Dissertation, Northwestern University, Evanston, IL.

Small M.K. and Nix W.D., (1992), 'Analysis of the accuracy of the bulge test in determining the mechanical properties of thin-films', J. Mater. Res. 7, 1553.

Vlassak J.J., (1994), 'New experimental techniques and analysis methods for the study of mechanical properties of materials in small volumes', Ph.D. Dissertation, Stanford University, Stanford, CA.

Xiang Y., Chen X., Vlassak J.J., (2005), 'Plane-strain bulge test for thin films', J. Materials Research Society, 20, pp.2360-2370.